Gaining an Atomistic Understanding of Auger-Meitner Recombination in Silicon

Kyle Bushick and Emmanouil Kioupakis
Department of Materials Science and Engineering, University of Michigan
Contact: kbushick@umich.edu

Background

Auger-Meitner recombination (AMR) is an intrinsic non-radiative recombination process in semiconductors.

AMR is of general interest due to its role in limiting the efficiency of solar cells,[1] LEDs,[2] and lasers,[3] among other devices.

The computational cost and complexity of calculating the AMR coefficient from first principles has precluded a detailed atomistic understanding of the full AMR mechanism in silicon.

$$\tau = \frac{n}{An + Bn^2 + Cn^3}$$

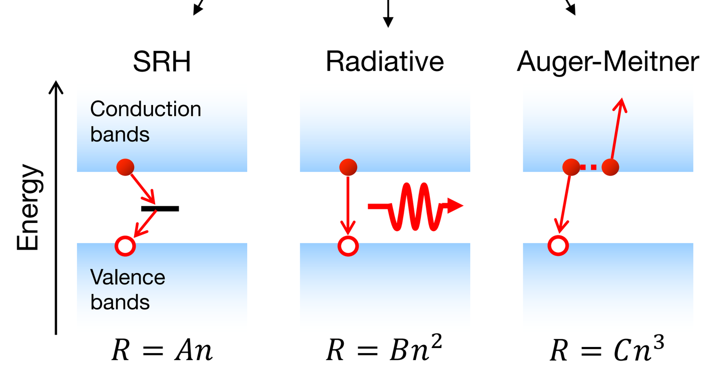

Figure 1: Different recombination mechanisms present in semiconductor materials

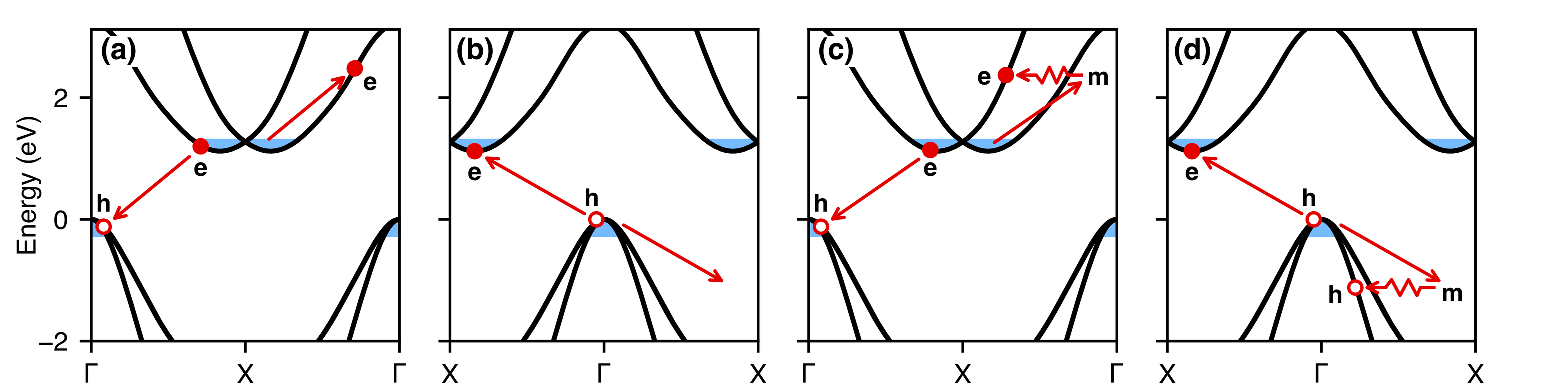

Figure 2: Schematic of the direct (a,b) and phonon-assisted (c,d) AMR process in silicon. The *eeh* process (a,c) promotes an electron while the *hhe* process promotes a hole to a higher energy state.

Methods

$$C = \frac{R}{Vn^3} = \frac{1}{\tau n^2}$$

$$R_{pa} = 2\frac{2\pi}{\hbar}\sum_{1234;\nu q} f_1 f_2 (1-f_3)(1-f_4)\left(n_{\nu q} + \tfrac{1}{2} \pm \tfrac{1}{2}\right) \times \left|\tilde{M}_{1234;\nu q}\right|^2 \delta(\epsilon_1 + \epsilon_2 - \epsilon_3 - \epsilon_4 \mp \hbar\omega_{\nu q})$$

$$R_{direct} = 2\frac{2\pi}{\hbar}\sum_{1234} f_1 f_2 (1-f_3)(1-f_4) \times |M_{1234}|^2 \delta(\epsilon_1 + \epsilon_2 - \epsilon_3 - \epsilon_4)$$

$$\tilde{M}^1_{1234;\nu q} = \sum_m \frac{g_{1m;\nu} M^d_{m234}}{\epsilon_m - \epsilon_1 \pm \hbar\omega_{\nu q} + i\eta}$$

W90

GNUparallel

Add implementation of HPC tools (MPI-IO, GNUparallel, hash tables) to improve computational efficiency

A direct run evaluates:
100,000 wavefunctions (>1 TB)
200,000,000 M_{1234} terms

A phonon-assisted run evaluates:
300,000 wavefunctions (>4 TB)
150,000,000 $\tilde{M}_{1234;\nu q}$ terms

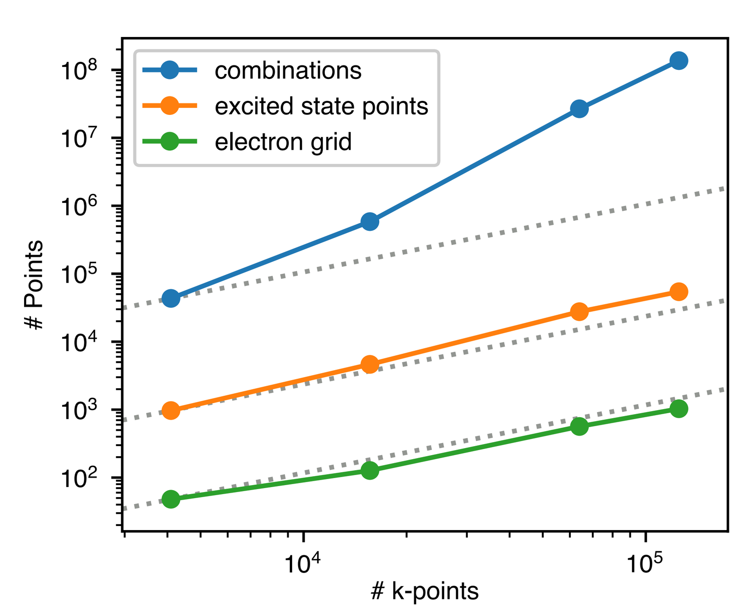

Figure 3: Scaling relation of calculation size with respect to Brillouin zone sampling grid.

Results

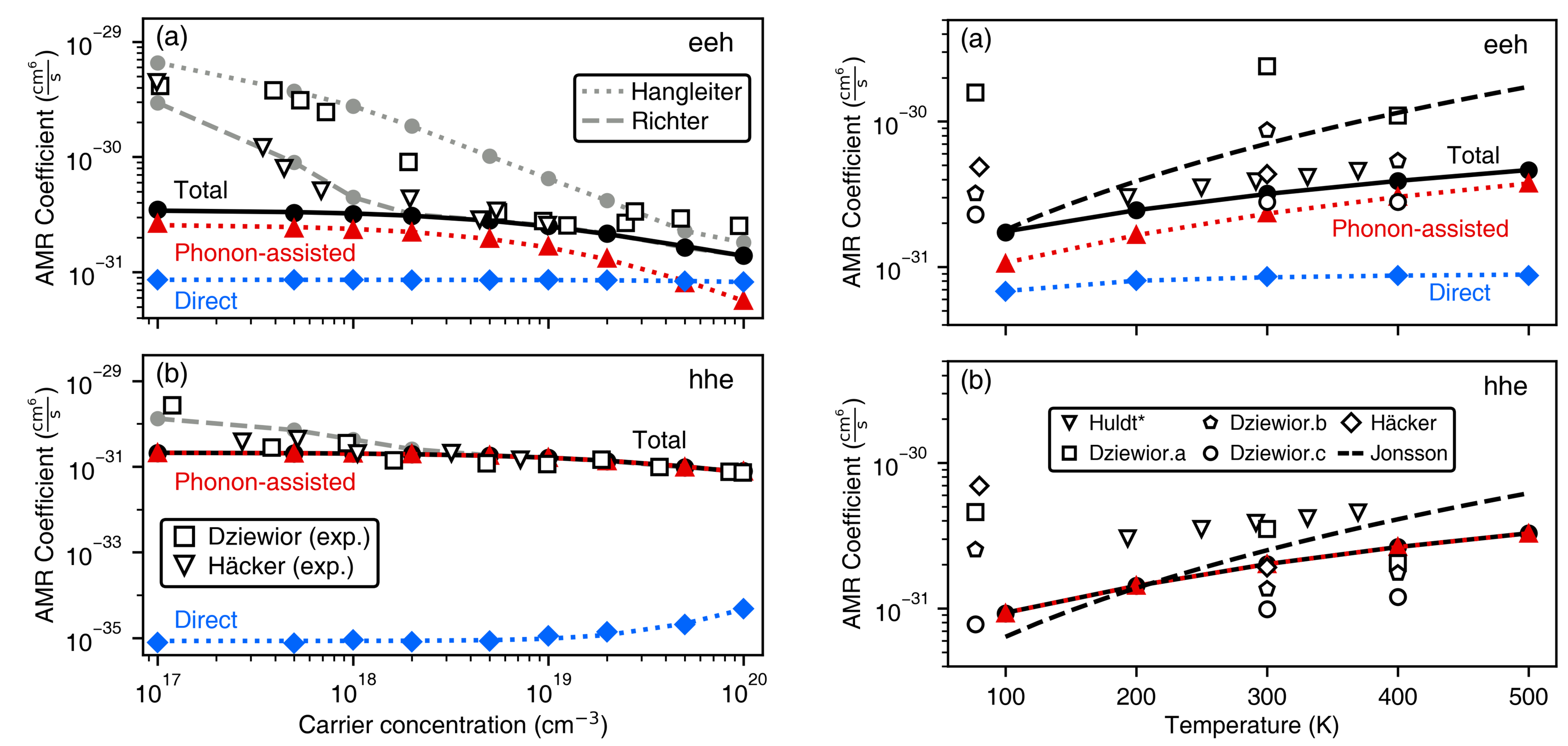

Figure 4: Carrier concentration (left) and temperature (right) dependence of the AMR coefficient. Experimental data points are included for reference.[4-7] At low carrier concentrations, we use models from literature to approximate Coulomb enhancement effects.[8,9]

$$C_{eeh}(n) = \frac{C^{eeh}_{dir}}{1 + \left(\frac{n}{n^*_{dir}}\right)^{\alpha}} + \frac{C^{eeh}_{pa}}{1 + \left(\frac{n}{n^*_{pa}}\right)^{\gamma}}$$

$$C_{eeh}(T) = C^{eeh}_{dir} e^{\frac{-E^{eeh}_a}{k_b T}} + \frac{C^{eeh}_{1,abs}}{e^{\frac{\hbar\omega_{low}}{k_b T}} - 1} + \frac{C^{eeh}_{2,abs}}{e^{\frac{\hbar\omega_{high}}{k_b T}} - 1} + C^{eeh}_{1,emit}\left(1 + \frac{1}{e^{\frac{\hbar\omega_{low}}{k_b T}} - 1}\right) + C^{eeh}_{2,emit}\left(1 + \frac{1}{e^{\frac{\hbar\omega_{high}}{k_b T}} - 1}\right)$$

We calculate both the free-carrier concentration and temperature dependence of AMR in silicon, showing excellent agreement with experiment. We construct physically motivated models for the AMR coefficient for general use.

Zone-edge acoustic phonons and perpendicular (*f*-type) low-energy electron configurations contribute most strongly to the overall AMR process. Excited free-carrier distributions help inform our understanding of the mechanisms.

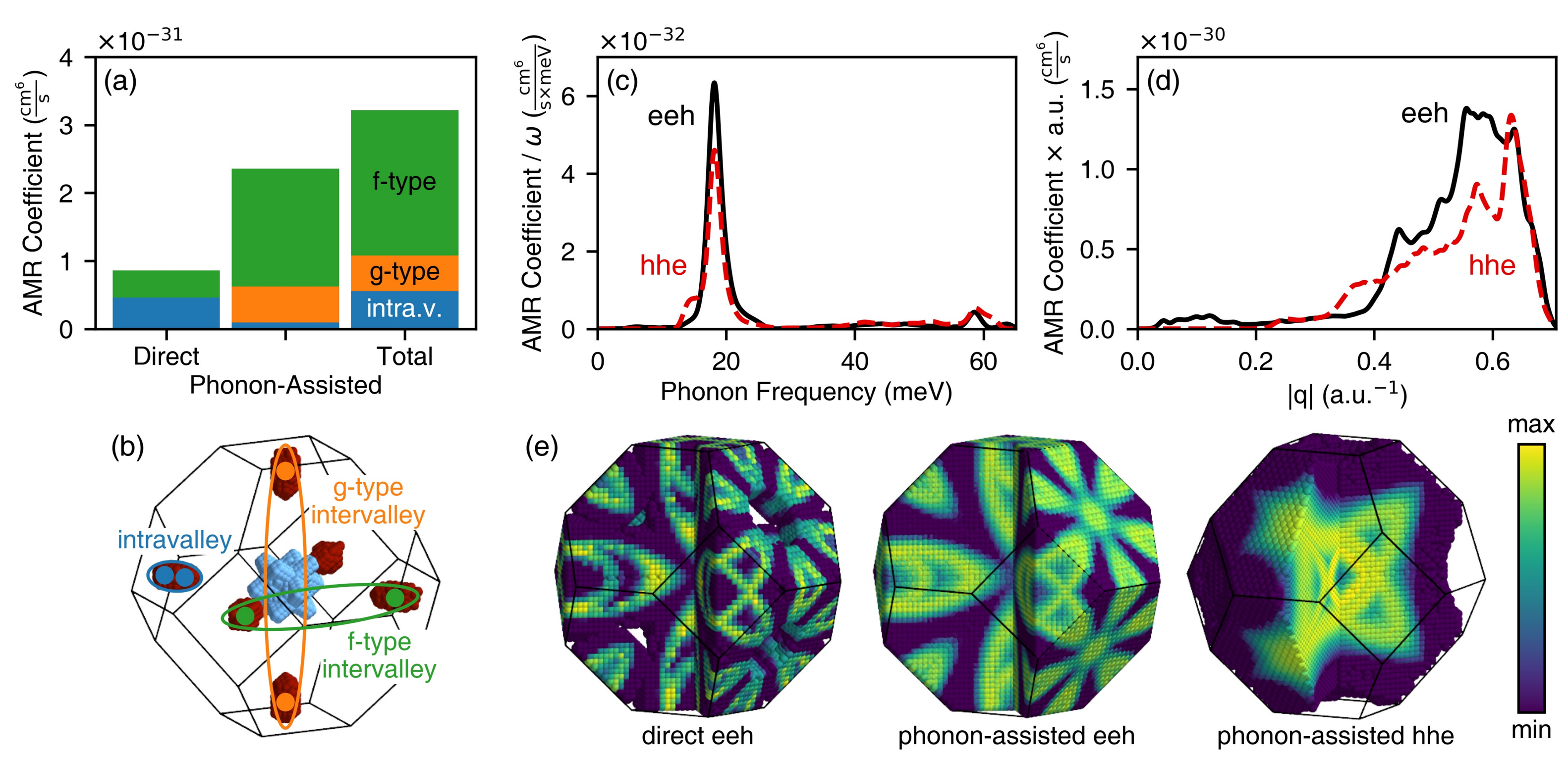

Figure 5: Decompositions of the total AMR rate reveal the atomistic details along different dimensions, including electronic valley configurations, phonon modes, and the excited free-carrier distributions.

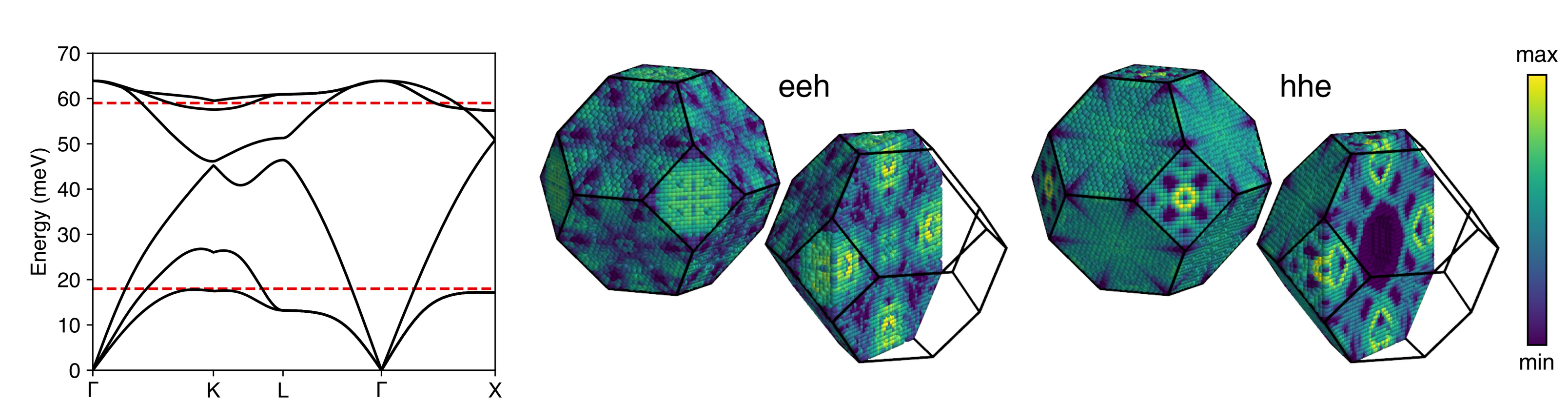

Figure 6: Visualization of the phonon dispersion along high symmetry lines (dotted lines at 18 and 59 meV are guides to the eye) and the distribution of phonon wave vectors that contribute to phonon-assisted AMR.

Conclusions

In this work, we perform the first calculation of both direct and phonon-assisted AMR in silicon from first principles. We demonstrate the importance of the phonon-assisted mechanism to both the *eeh* and *hhe* AMR processes.

Source	$C_{eeh,dir}$	$C_{eeh,pa}$	$C_{eeh,tot}$	$C_{hhe,dir}$	$C_{hhe,pa}$	$C_{hhe,tot}$
This work	**0.86**	**2.33**	**3.19**	**0.000089**	**2.0**	**2.0**
Govonoi (theory)[10]	~1.07	-	-	~0.000049	-	-
Dziewior (exp)[4]	-	-	2.8	-	-	0.99
Häcker (exp)[5]	-	-	4.35	-	-	2.02

Table 1: Comparison of AMR coefficients at T=300 K, n,p≈1 x 10^{18} cm^{-3}. Values are in units of 10^{-31} cm^6s^{-1}.

Future Work

Interpolation of Coulomb matrix elements:

$$M^d_{1234} \equiv \langle \psi_1 \psi_2 | W | \psi_3 \psi_4 \rangle \qquad M^x_{1234} \equiv \langle \psi_1 \psi_2 | W | \psi_4 \psi_3 \rangle$$

$$|M_{1234}|^2 \equiv \left|M^d_{1234} - M^x_{1234}\right|^2 + \left|M^d_{1234}\right|^2 + \left|M^x_{1234}\right|^2$$

Computational cost could be significantly reduced if we are able to interpolate the Coulomb matrix elements at arbitrary **k**-points. One challenge is that the Coulomb interaction is long-ranged in real space, so methods such as Wannier-like interpolation will not be feasible.

Investigate the effects of bi-axial strain on the AMR coefficient as a method to tune this recombination process, similar to other strain engineering efforts.

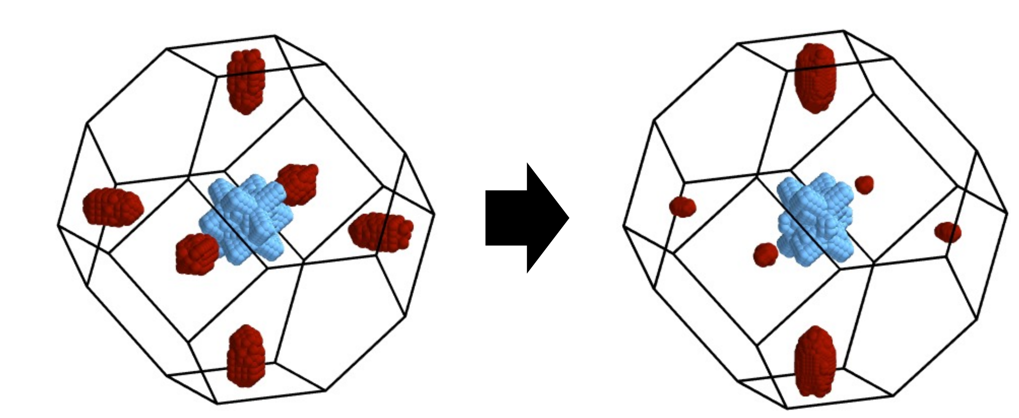

Figure 7: Effect of 1% bi-axial strain on the electron valley (red) occupation in silicon. The effect on holes (blue) is less dramatic.

Acknowledgements

The work is supported as part of the Computational Materials Sciences Program funded by the U.S. DOE, Office of Science, Basic Energy Sciences under Award No. DE-SC0020129. This work used resources of the National Energy Research Scientific Computing (NERSC) Center, a DOE Office of Science User Facility supported under Contract No. DE-AC02–05CH11231. K.B. acknowledges the support of the U.S. DOE, Office of Science, Office of Advanced Scientific Computing Research, Department of Energy Computational Science Graduate Fellowship under Award Number DE-SC0020347.

References

[1] M. J. Kerr, A. Cuevas, and P. Campbell, Progress in Photovoltaics: Research and Applications **11**, 97 (2003).
[2] Y. C. Shen, et al., Applied Physics Letters **91**, 141101 (2007).
[3] M. Takeshima, Journal of Applied Physics **58**, 3846 (1985).
[4] J. Dziewior and W. Schmid, Applied Physics Letters **31**, 346 (1977).
[5] R. Häcker and A. Hangleiter, Journal of Applied Physics **75**, 7570 (1994).
[6] L. Huldt, N. G. Nilsson, and K. G. Svantesson, Applied Physics Letters **35**, 776 (1979).
[7] P. Jonsson, H. Bleichner, M. Isberg, and E. Nordlander, Journal of Applied Physics **81**, 2256 (1997).
[8] A. Hangleiter and R. Häcker, Physical Review Letters **65**, 215 (1990).
[9] A. Richter, S. W. Glunz, F. Werner, J. Schmidt, and A. Cuevas, Physical Review B **86**, 165202 (2012).
[10] M. Govoni, I. Marri, and S. Ossicini, Physical Review B **84**, 075215 (2011).